OL | Organic Letters

pubs.acs.org/OrgLett Letter

Design and Synthesis of Near-Infrared Mechanically Interlocked Molecules for Specific Targeting of Mitochondria

Rabi Sankar Das, Pranab Chandra Saha, Nayim Sepay, Ayan Mukherjee, Sudipta Chatterjee, and Samit Guha*

Cite This: https://dx.doi.org/10.1021/acs.orglett.0c01922 Read Online

ACCESS | Metrics & More | Article Recommendations | Supporting Information

ABSTRACT: The entrapment of squaraine (SQ) within a molecular container to form rotaxane has been shown to improve the dye stability and the fluorescence proficiency inside the mitochondria. The macrocycle provides shelter and protects the near-infrared (NIR) SQ chromophore from nucleophilic attacks made by the exposed thiol of Cys-containing mitochondrial proteins and mitochondrial glutathione. Herein a microwave-assisted template-directed clipping reaction on low-loading 2-chlorotrityl chloride resin is used to develop an NIR unsymmetrical squaraine rotaxane in high quantum yield.

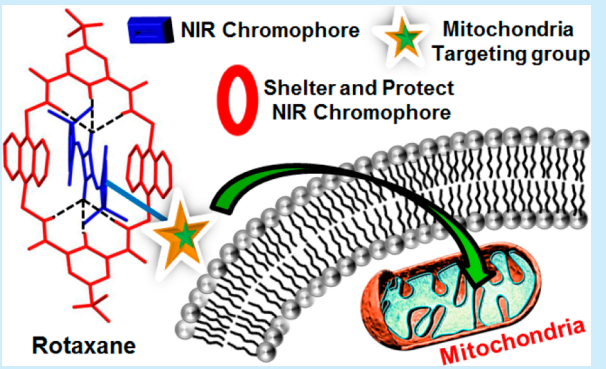

Using smart near-infrared (NIR) fluorescence imaging probes constructed from organic molecules to target specific cellular organelles is an emerging field of contemporary research.[1] NIR fluorescent biomarkers (650−900 nm) for intracellular locations are indispensable in contrast with visible and other fluorescent dyes because NIR light can permeate deep tissues and offers a meaningful bioimaging method with negligible autofluorescence background.[2] Mitochondria are crucial targets within the numerous cellular organelles.[3] Mitochondria are the powerhouse of cells, and they control cellular functions. The high negative inner mitochondrial membrane potential ($\Delta\Psi_m$ −150 to −180 mV) is distinctive because it does not exist in other cellular organelles, and this offers a design opportunity to target mitochondria. So far, squaraine (SQ) has been overlooked when building probes for the selective staining of mitochondria.[4] We envision that the electrophilic SQ chromophore could be susceptible to nucleophilic attack by the reactive thiols (SH) present in various mitochondrial proteins as well as mitochondrial glutathione (GSH), and hence NIR fluorescence could be quenched after the accumulation of SQ inside the mitochondria.[5] Moreover, SQ has a propensity to form nonfluorescent aggregates in an aqueous environment; this leads to substantial broadening of its absorption as well as emission bands, which is undesired for cellular organelle imaging.[6] These could be potential downsides for the development of SQ-based mitochondria tracking agents. We propose that the entrapment of a mitochondria-targeting SQ probe inside a container molecule to form mechanically interlocked molecules (rotaxane) that are stabilized through noncovalent interactions could be a method of improving the dye performance inside the mitochondria.[7] Smith and coworkers have made seminal contributions toward the development of squaraine rotaxane for various applications.[8] However, the synthesis of mitochondria targeting NIR unsymmetrical 1,3,3-trimethylindolin squaraine rotaxane is a challenging task. The synthesis of unsymmetrical SQRot can be achieved by the conventional oil-bath heating method, which takes days and often requires prolonged and difficult column chromatographic purification due to unwanted side products. Therefore, a fast, effective methodology with a high yield and product purity is required for the synthesis of unsymmetrical SQRot. We propose that microwave (MW)-assisted solid-phase synthesis on low-loading resin could be an effective way to construct an unsymmetrical rotaxane molecule. Moreover, the synthesized SQRot can be further bioconjugated with various target-specific functional groups, including organelle-selective targeting moieties. To the best of our knowledge, this is the first report of an NIR unsymmetrical 1,3,3-trimethylindoline squaraine-rotaxane-based mitochondria targeting and imaging agent.

We have designed and constructed an unsymmetrical 1,3,3-trimethylindoline SQ appended with triphenylphosphonium

Received: June 8, 2020

https://dx.doi.org/10.1021/acs.orglett.0c01922
Org. Lett. XXXX, XXX, XXX−XXX

(TPP$^+$) functionality (MSQ) to target mitochondria (Scheme 1).[9] A screening inspection is carried out under MW

Scheme 1. Synthesis of SQ-COOH and MSQ

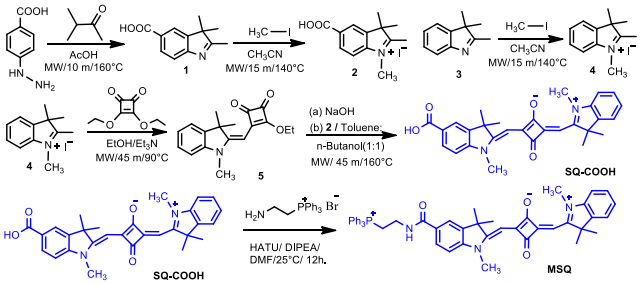

conditions to optimize the yield of the hemisquarate intermediate (**5**) from diethyl squarate (Table S3, Figures S6 and S7).[10] Compound **5** is hydrolyzed with NaOH and treated with **2** under MW irradiation to obtain unsymmetrical SQ with one −COOH functionality (SQ-COOH) (Table S4, Figures S8 and S9). The SQ-COOH is further conjugated with a TPP$^+$ functionality to get MSQ (Figures S10−S12).

The absorption and emission of MSQ are observed in the NIR region (Figure S22). A cellular uptake and imaging assay was performed by a confocal laser scanning microscope on an epithelioid cervix carcinoma HeLa cell line. In the case of mitochondria targeting MSQ, we observed a weak NIR fluorescence signal inside the mitochondria (Figure 1a, Figure

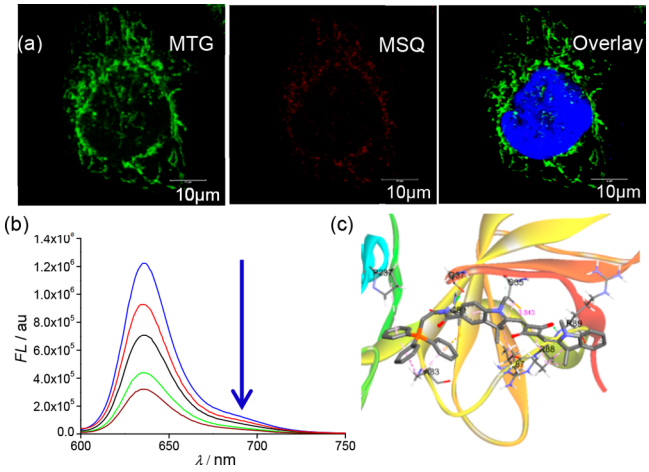

Figure 1. (a) Confocal images of MSQ colocalized with MitoTracker Green (MTG) in HeLa cells. (b) A decrease in the fluorescence intensity of MSQ (2 μM in DMSO/pH 8 buffer solution (1:10)) is observed on the gradual addition of GSH (2 μM) at mitochondrial pH 8. (c) Docking poses of MSQ with the exposed Cys (C35) containing mitochondrial protein ATP synthase subunit beta 1.

S23). We hypothesize that the MSQ is selectively incorporated inside the mitochondria; however, the chromophore is vulnerable to nucleophilic attack by the exposed Cys-containing mitochondrial proteins as well as mitochondrial GSH. This leads to a discontinuity in conjugation, and thus the NIR fluorescence of MSQ is dropped. To understand the fluorescence turn-off of MSQ by the nucleophilic attack of the −SH group, we used 2-mercaptoethanol with 1 equiv of Hunig's base in DMSO as well as GSH in mitochondrial pH 8.0 as model systems.[5] We treated a DMSO/pH 8.0 buffer solution (1:10) of MSQ with GSH. Within a few minutes, the blue color of MSQ disappeared after the addition of GSH or 2-mercaptoethanol. UV/vis and fluorescence titration of MSQ in the presence of GSH and 2-mercaptoethanol showed bleaching of the λ_{abs} as well as λ_{em} (Figure 1b and Figures S24 and S25). The molecular docking of MSQ with Cys exposed mitochondrial protein ATP synthase subunit beta 1 (PDB: 4Q4L), and other SH-exposed proteins showed interactions between the SH moieties and MSQ (Figure 1c, Figure S26). The encapsulation of MSQ dye inside a molecular container has been shown to greatly improve the MSQ chemical stability and also alter the fluorescence spectroscopic and microscopic properties.

Herein the SQ-COOH molecule is loaded on a low-loading 2-chlorotrityl chloride (2-CTC) resin through −COOH.[11] Efforts to synthesize the rotaxane molecule through a direct slippage method in solution are ineffective. A template-directed clipping reaction on 2-CTC resin is used to transform SQ-COOH to SQRot-COOH under MW conditions (Scheme 2).[12] Most strikingly, the unwanted side products of the

Scheme 2. Synthesis of Unsymmetrical SQRot-COOH Using the MW-Assisted Solid-Phase Protocol on 2-CTC Resin and the Construction of MSQRot

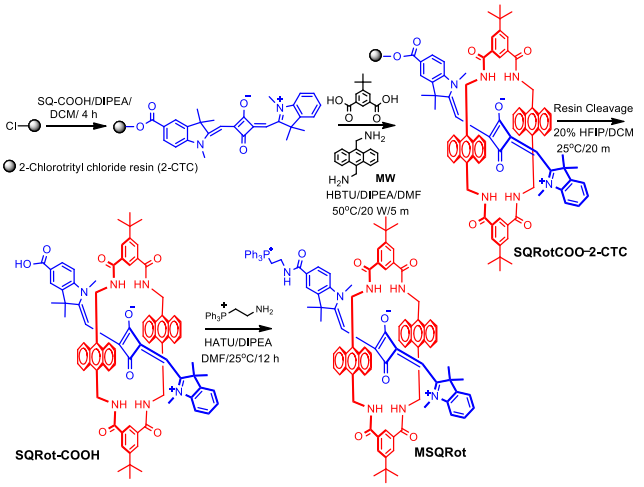

conventional synthesis, whose formation is the most major drawback of rotaxane construction, can be easily removed in the solid phase by following the washing steps with suitable solvents. Eventually, the desired rotaxane is obtained from the resin support. The SQRot-COOH is cleaved from the 2-CTC resin and further conjugated with TPP$^+$ functionality to obtain MSQRot (Scheme 2). Here MSQRot consists of an unsymmetrical SQ chromophore as an NIR imaging signaling unit tethered with a lipophilic cationic TPP$^+$ group to target mitochondria and a macrocycle to shelter and protect the chromophore from nucleophilic attack inside the mitochondria. The unsymmetrical MSQRot is acquired in satisfactory yield and is characterized by numerous spectroscopic techniques (Figures S13−S15). MSQRot displays one ^{31}P NMR peak at 24.8 ppm for the TPP$^+$ group. A control symmetrical rotaxane (SQRot) lacking the TPP$^+$ moiety is also synthesized (Figures S18−S21).

The changes in ^{1}H NMR chemical shifts caused by MSQRot formation have been compared with the free macrocycle and MSQ (Figure 2a). Most notable is the extreme downfield shift for macrocycle proton "C" and "NH" due to hydrogen bonding

https://dx.doi.org/10.1021/acs.orglett.0c01922
Org. Lett. XXXX, XXX, XXX−XXX

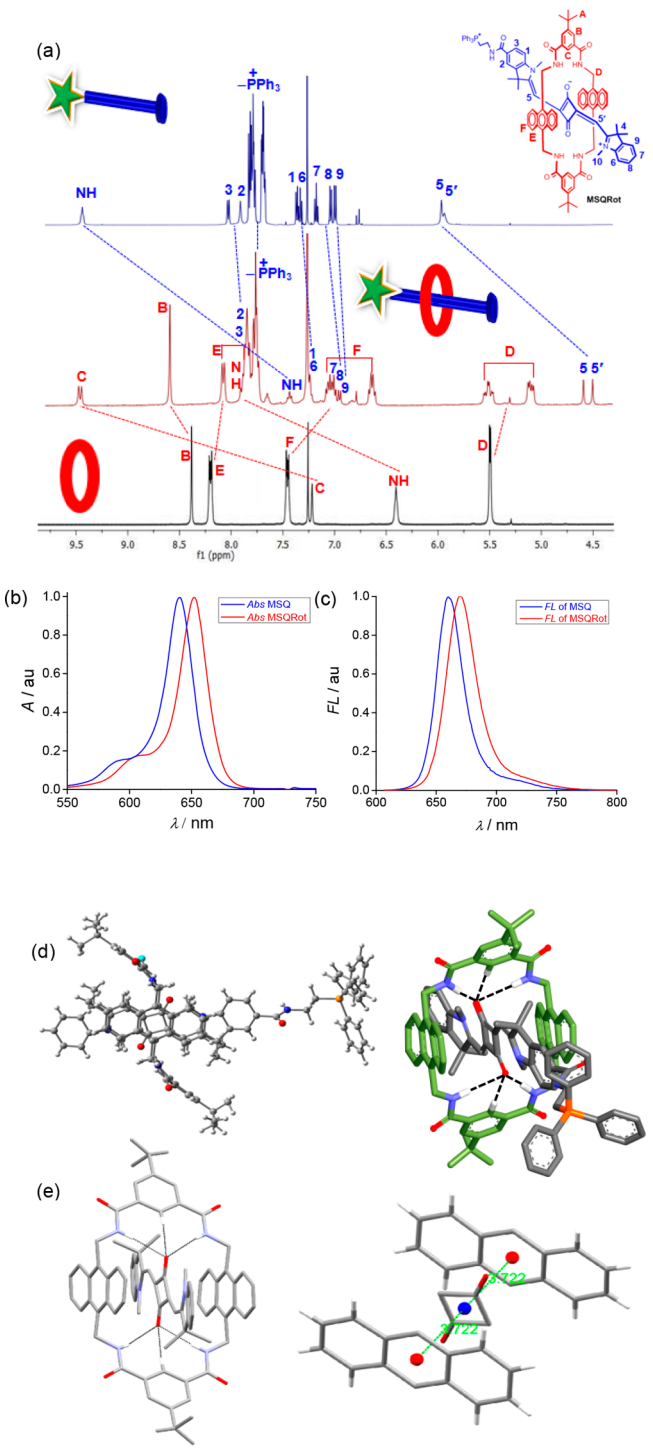

Figure 2. (a) Partial ^{1}H NMR stacking of the free macrocycle, MSQRot, and MSQ in $CDCl_3$. (b) Normalized absorption plot of MSQ (2 μM) and MSQRot (2 μM) in $CHCl_3$. (c) Normalized fluorescence plot of MSQ (2 μM) and MSQRot (2 μM) in $CHCl_3$. Absorption and emission plots showing the bathochromic shift for rotaxane formation. (d) B3LYP/6-31+G** energy-minimized structure of MSQRot. (e) Single-crystal X-ray structure of control SQRot. The centroid-to-centroid distance between the anthracene residues and the C_4O_2 core is 3.7 Å.

with SQ O atoms. Moreover, an upfield shift of macrocyclic protons E and F is observed for rotaxane formation. For MSQRot, the anthracene residues of the macrocycle create anisotropic shielding zones for the 5,5′ (two well-separated singlet) protons of the MSQ, and hence an upfield shift in ^{1}H NMR is observed. The B3LYP/6-31+G** energy-minimized structure shows that the two 1,3,3-trimethylindolin rings of MSQ are in the trans configuration in the encapsulated form of MSQRot (Figure 2d, Figure S27). Tetralactam N−H bonds and two C−H bonds of the phenyl ring of the macrocycle are forming hydrogen bonds with two O atoms of the C_4O_2 residue of MSQ. The central C_4O_2 core of MSQ, which is highly electron-deficient and sandwiched between the two electron-rich anthracene moieties (centroid-to-centroid, anthracene residues to C_4O_2 ring, distance is 3.9 Å), is stabilized through a D−A−D-type interaction and thus is expected to block nucleophilic attacks. We are fortunate to obtain the single-crystal X-ray structure of the control symmetrical SQRot molecule lacking the TPP^+ group, which also exhibited a trans orientation similar to that of the *N*-methyl indoline residues (Figure 2e, Figure S28, Table S5). Four N−H bonds and two phenyl C−H bonds of the macrocycle are forming hydrogen bonds with SQ O atoms (N−H···O as well as C−H···O hydrogen-bond distance is ca. 2.3 Å). The C_4O_2 core is also forming D−A−D-type interactions with two anthracene residues (D−A distance 3.7 Å) in SQRot. Also, the λ_{abs} and λ_{em} of MSQRot show a characteristic bathochromic shift ca. 12 nm from the original spectra of MSQ in $CHCl_3$ (Figure 2b,c). The absorption spectra of unsymmetrical MSQRot revealed an intense peak (λ_{max}) at 652 nm in $CHCl_3$ with a large molar extinction coefficient of 1.5×10^5 M^{-1} cm^{-1} (Table S6). The λ_{em} of MSQRot is observed to be 670 nm in $CHCl_3$. There is a 3.5-fold augmentation in the MSQRot quantum yield ($(\Phi_f)_{MSQRot}$ = 0.53) in comparison with MSQ ($(\Phi_f)_{MSQ}$ = 0.15) in DMSO, which is due to the reduced rotational and vibrational motions of the entrapped MSQ and because the consequent nonradiative excited-state relaxation pathways are the least feasible.[13] The anthracene fluorescence at λ_{ex} 365 nm becomes weaker for MSQRot formation in comparison with the free macrocycle due to FRET from anthracene to the trapped MSQ (Figure S29).

Dethreading could be a potential drawback of rotaxane located inside the subcellular organelles.[14] ^{1}H NMR studies in $CDCl_3$ at 37 °C for 2 days showed no dissociation of the MSQ from MSQRot. The mechanical stability of MSQRot is also investigated by absorption/emission spectroscopy in $CHCl_3$. There is no evidence of MSQRot dethreading after 48 h at 37 °C. This confirmed that the gem-dimethyl and *N*-methyl groups in 1,3,3-trimethylindoline residues and the TPP^+ group are bulky enough to prevent MSQRot dethreading. The plausible biological interference from GSH at mitochondrial pH 8 at 37 °C is inspected over 48 h. No significant emission changes in MSQRot are perceived in GSH at pH 8 (Figure S30). Cell viability studies show that the MSQRot is less toxic to HeLa carcinoma and the noncancerous HEK293 cell line (Figure S31). The outstanding biocompatibility, insignificant cytotoxicity, narrow NIR absorption/emission band, and high quantum yield further make the MSQRot a smart choice for organelle staining. To confirm the mitochondrial selectivity, a colocalization test involving MSQRot is executed in HeLa and A549 carcinoma cells with a mitochondria specific marker, MitoTracker Green (MTG). The MSQRot displayed decent colocalization with MTG in the confocal microscopy with a Pearson's correlation (PC) coefficient of 0.89 for HeLa and 0.85 for A549 (Figure 3 and Figures S32 and S33). The accumulation of MSQRot in the mitochondria is anticipated to be 500−1000 times greater than that in the extracellular region

https://dx.doi.org/10.1021/acs.orglett.0c01922
Org. Lett. XXXX, XXX, XXX−XXX

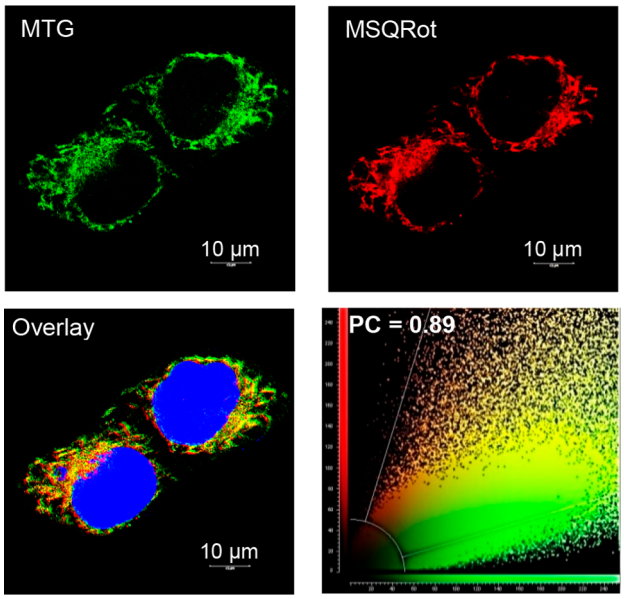

Figure 3. Confocal images of MSQRot colocalized with MTG in HeLa cells. The colocalization scatter plot shows PC coefficient: 0.89.

due to the potential gradient ($\Delta\Psi_m$ −150 to −180 mV vs plasma membrane potential −30 to −60 mV).[9] The inner mitochondrial concentrations of MSQRot in HeLa cells are determined by fluorescence analysis to be 1.3 ± 0.3 mM and 4.2 ± 0.6 mM, which are greater than the original exterior concentrations of 2 and 5 μM, respectively (Figure S34). The mitochondrial target selectivity of MSQRot is compared with a control symmetrical SQRot lacking the TPP^+ functionality. SQRot stains inside the A549 cells; however, confocal images show that it is poorly colocalized with mitochondria tracker MTG (Figure S35).

In summary, the macrocycle gives shelter and protects the MSQ dye from nucleophilic attack inside the mitochondria. This rotaxane molecule can be functionalized to target specific cellular organelles. MSQRot with an appended targeting TPP^+ group could be an effective molecular probe for mitochondrial therapy with NIR imaging diagnostics.

■ ASSOCIATED CONTENT

Supporting Information

The Supporting Information is available free of charge at https://pubs.acs.org/doi/10.1021/acs.orglett.0c01922.

Experimental procedures, synthesis and characterization, crystallographic data, computational results, and confocal images (PDF)

Accession Codes

CCDC 1998840 contains the supplementary crystallographic data for this paper. These data can be obtained free of charge via www.ccdc.cam.ac.uk/data_request/cif, or by emailing data_request@ccdc.cam.ac.uk, or by contacting The Cambridge Crystallographic Data Centre, 12 Union Road, Cambridge CB2 1EZ, UK; fax: +44 1223 336033.

■ AUTHOR INFORMATION

Corresponding Author

Samit Guha − *Department of Chemistry, Organic Chemistry Section, Jadavpur University, Kolkata 700032, India;* orcid.org/0000-0001-6643-9882; Email: samitfsu@gmail.com, samit.guha@jadavpuruniversity.in

Authors

Rabi Sankar Das − *Department of Chemistry, Organic Chemistry Section, Jadavpur University, Kolkata 700032, India*

Pranab Chandra Saha − *Department of Chemistry, Organic Chemistry Section, Jadavpur University, Kolkata 700032, India;* orcid.org/0000-0003-4808-1375

Nayim Sepay − *Department of Chemistry, Organic Chemistry Section, Jadavpur University, Kolkata 700032, India;* orcid.org/0000-0001-7702-3989

Ayan Mukherjee − *Department of Chemistry, Organic Chemistry Section, Jadavpur University, Kolkata 700032, India*

Sudipta Chatterjee − *Department of Chemistry, Serampore College, Serampore, West Bengal 712201, India;* orcid.org/0000-0002-3273-1751

Complete contact information is available at: https://pubs.acs.org/10.1021/acs.orglett.0c01922

Notes

The authors declare no competing financial interest.

■ ACKNOWLEDGMENTS

This work is supported by DST-SERB, Govt. of India (file no. ECR/2017/001405).

■ REFERENCES

(1) (a) Zhu, H.; Fan, J.; Du, J.; Peng, X. *Acc. Chem. Res.* **2016**, *49*, 2115−2126. (b) Wang, L.; Frei, M. S.; Salim, A.; Johnsson, K. *J. Am. Chem. Soc.* **2019**, *141*, 2770−2781.

(2) (a) Yan, R.; Hu, Y.; Liu, F.; Wei, S.; Fang, D.; Shuhendler, A. J.; Liu, H.; Chen, H.-Y.; Ye, D. *J. Am. Chem. Soc.* **2019**, *141*, 10331−10341. (b) Ducharme, G. T.; LaCasse, Z.; Sheth, T.; Nesterova, I. V.; Nesterov, E. E. *Angew. Chem., Int. Ed.* **2020**, *59*, 8440−8444.

(3) Liew, S. S.; Qin, X.; Zhou, J.; Li, L.; Huang, W.; Yao, S. Q. *Angew. Chem., Int. Ed.* **2020**, DOI: 10.1002/anie.201915826.

(4) Babu, P. S. S.; Manu, P. M.; Dhanya, T. J.; Tapas, P.; Meera, R. N.; Surendran, A.; Aneesh, K. A.; Vadakkancheril, S. J.; Ramaiah, D.; Nair, S. A.; Pillai, M. R. *Sci. Rep.* **2017**, *7*, 42126.

(5) (a) Hewage, H. S.; Anslyn, E. V. *J. Am. Chem. Soc.* **2009**, *131*, 13099−13106. (b) Arunkumar, E.; Forbes, C. C.; Noll, B. C.; Smith, B. D. *J. Am. Chem. Soc.* **2005**, *127*, 3288−3289. (c) Anees, P.; Sreejith, S.; Ajayaghosh, A. *J. Am. Chem. Soc.* **2014**, *136*, 13233−13239.

(6) Chen, H.; Farahat, M. S.; Law, K.-Y.; Whitten, D. G. *J. Am. Chem. Soc.* **1996**, *118*, 2584−2594.

(7) (a) Stoddart, J. F. *Angew. Chem., Int. Ed.* **2017**, *56*, 11094−11125. (b) Craig, M. R.; Hutchings, M. G.; Claridge, T. D. W.; Anderson, H. L. *Angew. Chem., Int. Ed.* **2001**, *40*, 1071−1074. (c) Lee, S.; Chen, C.-H.; Flood, A. H. *Nat. Chem.* **2013**, *5*, 704−710.

(8) (a) Johnson, J. R.; Fu, N.; Arunkumar, E.; Leevy, W. M.; Gammon, S. T.; Piwnica-Worms, D.; Smith, B. D. *Angew. Chem., Int. Ed.* **2007**, *46*, 5528−5531. (b) Jarvis, T. S.; Collins, C. G.; Dempsey, J. M.; Oliver, A. G.; Smith, B. D. *J. Org. Chem.* **2017**, *82*, 5819−5825. (c) Gassensmith, J. J.; Arunkumar, E.; Barr, L.; Baumes, J. M.; DiVittorio, K. M.; Johnson, J. R.; Noll, B. C.; Smith, B. D. *J. Am. Chem. Soc.* **2007**, *129*, 15054−15059.

(9) Zielonka, J.; Joseph, J.; Sikora, A.; Hardy, M.; Ouari, O.; Vasquez-Vivar, J.; Cheng, G.; Lopez, M.; Kalyanaraman, B. *Chem. Rev.* **2017**, *117*, 10043−10120.

(10) Barbero, N.; Magistris, C.; Park, J.; Saccone, D.; Quagliotto, P.; Buscaino, R.; Medana, C.; Barolo, C.; Viscardi, G. *Org. Lett.* **2015**, *17*, 3306−3309.

(11) López-Macià, A.; Jiménez, J. C.; Royo, M.; Giralt, E.; Albericio, F. *J. Am. Chem. Soc.* **2001**, *123*, 11398−11401.

(12) Leigh, D. A.; Murphy, A.; Smart, J. P.; Slawin, A. M. Z. *Angew. Chem., Int. Ed. Engl.* **1997**, *36*, 728−732.
(13) Collins, C. G.; Baumes, J. M.; Smith, B. D. *Chem. Commun.* **2011**, *47*, 12352−12354.
(14) Carrasco-Ruiz, A.; Tiburcio, J. *Org. Lett.* **2015**, *17*, 1858−1861.

https://dx.doi.org/10.1021/acs.orglett.0c01922
Org. Lett. XXXX, XXX, XXX−XXX